INSTITUTO SUPERIOR TÉCNICO
Universidade Técnica de Lisboa

Non-Linear Static Analyses on Bridges Equipped with Viscous Dampers

The Case of the Padre Cruz Viaduct – North-South Axis, Lisbon

João Maria Henriques Pires de Matos

Extended Abstract

Dissertation towards the Masters Degree in

Civil Engineering

October 2009

1. Introduction and Aims

The aim of this study is to make a set of non-linear static analyses. These analyses provide information on the ductility of the structure, since they enable the yield and collapse of the structural elements to be traced sequentially in a graphic that represents the whole structure, thus allowing critical areas that require more detailed dimensioning to be identified, avoiding the use of the behaviour coefficient, normally equal for all the structural elements.

With the development of technology, devices have appeared called viscous dampers, which enable the dissipation of energy in structures to be increased when subjected to seismic activity, minimising the damage caused to structural elements.

This study is intended to develop a methodology for non-linear static analyses of bridges equipped with viscous dampers when subject to seismic activity. Although static, these analyses should reflect the dynamic contribution of the devices.

This methodology will be applied to a specific case: the Padre-Cruz Viaduct (North-South Axis, Lisbon), because this structure does have devices of this type.

Finally, we wanted to use the results of the non-linear static analyses in such a way as to predict the probability of the structure sustaining a certain level of damage when under a given earthquake loading, thereby providing a reference result prior to performing a detailed analysis.

2. Description Padre Cruz Viaduct

The structure to be studied, the “North/South Road Axis viaduct over Avenida Padre Cruz”, was promoted by the IEP (Portuguese Highways Institute), more specifically by the Área Funcional de Obras de Arte e Estruturas Especiais within IEP, and it was designed by the company JSJ.

The viaduct has a length of 770m between the bearing axes at the abutments and this is subdivided into 11 spans, the division of the spans being made by a set of 10 pillars and 2 abutments.

Abutment E1 is the junction linking the North/South Road Axis (Telheiras) and the Viaduct.

Abutment E2 establishes the link between the Viaduct and the IP7. Throughout the IP7 there are various exits from the city of Lisbon to other destinations, such as the Vasco da Gama bridge, the A1 North and the A8.

Figure 1 shows a diagram giving a better understanding of the distribution of spans.

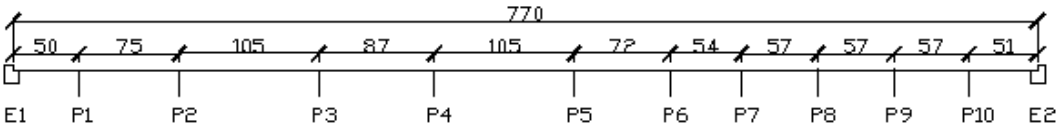

Fig. 1 - Distribution of spans on the Padre Cruz viaduct

Between abutment E1 and pillar P3 the longitudinal axis makes a shallow curve of constant radius.

As for the geometry of the transverse section of the deck, this section is formed by a single-cell box girder 32.4m wide. This width is achieved at the expense of transverse flat lattice-work resting on the box girder, at 3 metre spaces longitudinally. The following table shows the geometrical quantity values of the section, which provides an understanding of the longitudinal inertia variation of the deck.

vão		de extremidade		tipo		de transição		grande	
		50.0 e 51.0m		54.0 e 57.0m		72.0 e 75.0m		87.0 e 105.0m	
secção		vão	Apoio (encontro)	vão	Apoio	vão	Apoio	vão	Apoio
h		2.70	2.70	2.70	2.70	2.70	2.70	2.70	5.10
$e_{banzo,inferior}$		0.30	0.70	0.30	0.70	0.30	0.70	0.30	1.35
$e_{banzo,superior}$		0.36	0.36	0.36	0.36	0.36	0.36	0.36	0.36
e_{alma}		0.40	1.00	0.40	1.20	0.40	0.40	0.50	1.20
A_m	c/sobreelev.	18.7	24.2	18.7	24.7	18.7	24.7	19.0	34.9
	s/sobreelev	18.3	-	18.3	24.1	18.3	24.1	18.6	34.1
I	c/sobreelev.	16.9	23.9	16.9	24.0	16.9	24.0	17.2	128.6
	s/sobreelev	14.0	-	14.0	19.5	14.0	19.5	14.2	114.9
y_g	c/sobreelev.	0.78	1.04	0.78	1.05	0.78	1.05	0.79	2.30
	s/sobreelev	0.94	-	0.94	1.18	0.94	1.18	0.95	2.42

The geometry of the viaduct pillars is obtained by two irregular hexagons linked by a rectangular web.

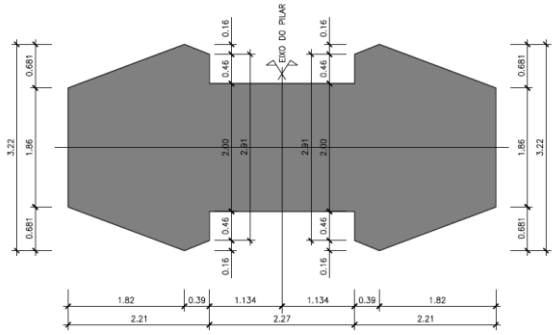

Fig. 2 - Geometry of the viaduct pillars

The deck is connected to the pillars by pot-type bearings, two per pillar where the cores of the cross section of the deck rest. These bearings are divided into two groups, group A and group B.

- Group A – Bearings with rigid transverse bracing and free displacement along the longitudinal axis of the deck on pillars P1, P2, P3, P6, P7, P8, P9, P10, E1, E2;
- Group B – Bearings with rigid bracing in both directions on pillars P4 and P5;

Four seismic dampening viscous dampers were also placed at each abutment, and these are grouped in sets of two centred on the webs of the box and the abutment uprights.

3. Modelling of the Padre Cruz Viaduct

The modelling of the viaduct was carried out using *SAP2000 software*. Frame elements were used to model the whole structure. The deck and the pillars were modelled with a set of 3 metre long members in the case of the deck and 1 metre long in the case of the pillars. The geometric properties of member sections were the same as for the geometric properties of the physical sections.

The modelling of the depth of the foundation was calculated based on the model of isolated shoe plates seated on soil composed of miocenic formations.

To model the linking of the deck to the pillars, dissipation was applied to a set of rigid bars in order to ensure that the computer model could represent the existing deck-pillar connections.

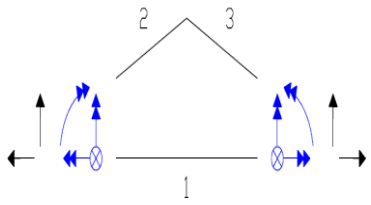

Fig. 3 - Group A releases

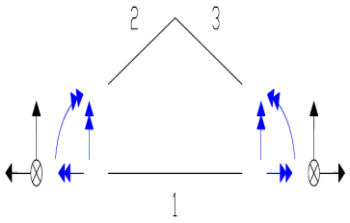

Fig. 4 - Group B releases

In figures 3 and 4, stress releases applied on the extremity of bar 1 is shown in blue. The stresses in black were not released.

4. Measurement Tests

A set of three measurement tests were made to determine the vibration frequencies of the structure and to compare the results of these frequencies with those obtained from the computer model. The places where the tests were carried out are shown in the following figure.

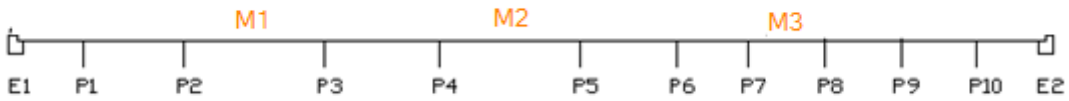

Fig 5 - Places where the tests were carried

The following table shows the values obtained from the measurement tests and those obtained from the computer model.

Modes of Vibration from computer model					Frequencies measured								
					M1 Trial			M2 Trial			M3 Trial		
Mode	F	UX	UY	UZ	F [Hz]			F [Hz]			F [Hz]		
	Hz	%	%	%	X	Y	Z	X	Y	Z	X	Y	Z
1	0.70	1.96%	0.00%	1.48%	0.70								
2	0.93	0.24%	0.00%	0.15%	0.89		0.89			0.89			
3	1.04	65.43%	1.16%	0.22%	1.09		1.11		1.07	1.07			
4	1.05	1.42%	47.39%	0.01%		1.09							
5	1.30	0.00%	9.60%	0.00%									
6	1.41	15.99%	0.01%	0.18%	1.47								
7	1.56	1.49%	0.02%	0.54%	1.53		1.55	1.56					1.54
8	1.56	0.00%	21.03%	0.00%		1.55							
9	1.71	5.13%	0.00%	0.05%	1.77			1.72			1.76		
10	1.81	0.45%	0.00%	13.26%			1.87			1.78			1.75

Tab. 1 - Values of vibration frequencies

5. Non-Linear Model

In order for the analysis to be non-linear, non-linear characteristics of critical sections would have to be introduced into the model. As these types of structures present a gantry-type behaviour, deformations in the viaduct occur due to bending stresses. So the constitutive relations that characterise the non-linear behaviour of the critical sections are of the Moment – Curvature type. As analyses are only carried out in this study for the horizontal direction, the critical sections are located at the base and at the top of the pillars.

For the constitutive relations of the critical sections to be obtained, first the constitutive relations of the materials that comprise these sections had to be defined.

The materials that make up the sections of the pillars are identified in the following table. Note that average values of the yield point were used to define the constitutive relation of all the materials since this study wishes to analyse the behaviour of the structure and not take dimensioning measurements.

Material	Average yield Stress
C30/37	38 Mpa
C40/50	48 Mpa
A500NR	585 Mpa

Tab 2 - Average Stress values

As the analysis to be carried out was static, the constitutive relations of the materials were defined accepting that these would be submitted to a monotonic loading.

The stress-strain relation of the steel rods was obtained using the theory developed by Pipa, M. J. A. L., [1993], in which the behaviour of the steel is in three phases:

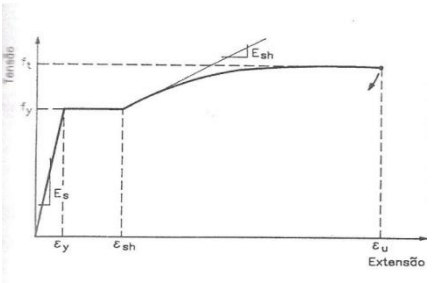

Fig. 6- Steel Stress - Strain model

- Elastic region $(0 \leq \varepsilon_s \leq \varepsilon_{ym})$

  $f_s = E_s \varepsilon_s$

- Yield threshold $(\varepsilon_{ym} \leq \varepsilon_s \leq \varepsilon_{sh})$

  $f_s = f_{ym}$

- Hardening region $\varepsilon_{sh} \leq \varepsilon_s \leq \varepsilon_{su}$

  $$f_s = f_{su} + (f_{ym} - f_{su}) \left[\frac{\varepsilon_{su} - \varepsilon_s}{\varepsilon_{su} - \varepsilon_{sh}} \right]^p$$

In the definition of the stress - strain of concrete, the only consideration applied was that of its resistance to compression and the theory defined by Mander, J. B., [1988] was followed, similar to that represented in EC8 part 2. This constitutive relation takes into account the confinement effect of concrete and is shown in figure 7.

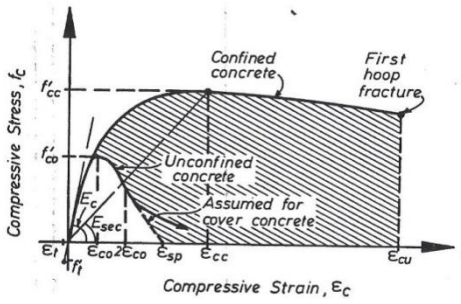

Fig 7 - Stress - Strain model for confined concrete

The constitutive relation of a section of concrete that is confined and subject to a monotonic loading is as follows:

$$f_c = \frac{f`_{cc} x r}{r - 1 + x^r}$$

In which:

- $f`_{cc}$ is the compressive stress of the confined concrete;
- $x = \frac{\varepsilon_c}{\varepsilon_{cc}}$, ε_c is the longitudinal strain of the concrete;
- $\varepsilon_{cc} = \varepsilon_{co}\left[1 + 5\left(\frac{f`_{cc}}{f_{cm}} - 1\right)\right]$ strain of the confined concrete;
- $r = \frac{E_c}{E_c + E_{sec}}$; $E_c = 5000\sqrt{f_{cm}}$ in MPa ; $E_{sec} = \frac{f`_{cc}}{\varepsilon_{cc}}$;
- $\varepsilon_{co} = 0{,}002$

To determine the constitutive relation of a section of the pillars, an iterative programme in Excel was used which took as its base the following calculation flowchart:

1. Divide the section into 80 bands of equal thickness ($i =$ band number);
2. Determine the quantity of Reinforcement (A_{si}) and Concrete (A_{ci}) in each band
3. Determine the position of the centre of gravity of each band $y_{Gi} = \frac{h(80 - i + 0{,}5)}{80}$
4. Calculate the strain in the centre of gravity of the band based on the strain on the top fibre of the concrete and according to the curvature $\varepsilon_i = \varepsilon_{sup} - (h - y_{Gi})\chi$

   (NOTE: ε_{sup} will be increased and χ is the variable to be determined)
5. From the constitutive relations the stresses of the materials in the bands f_{si} e f_{ci} are calculated
6. Calculate the forces in each band $F_{si} = f_{si} \times A_{si}$ e $F_{ci} = f_{ci} \times A_{ci}$

7. Determine the curvature so that the sum of the forces on the bands is equal to the normal force of gravitational loads applied to the section $\sum_{i=1}^{80} F_{si} + F_{ci} = N_d$

8. Once the curvature is known, the corresponding moment needs to be determined

$$M_G = \sum_{i=1}^{80} F_i \left(y_{Gi} - \frac{h}{2}\right) \text{ where } F_i = F_{si} + F_{ci}$$

9. A point of moment - curvature is thus found, and the process is repeated for another value of ε_{sup}

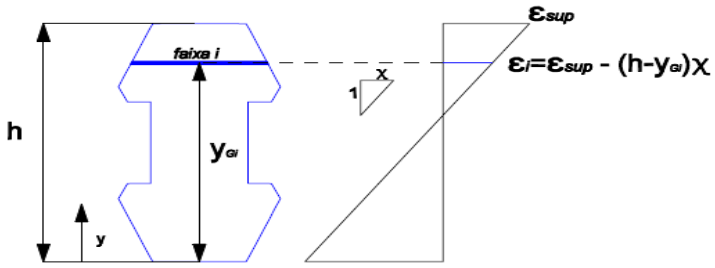

Fig. 8- Example of the strain diagram

6. Non-Linear Static Analysis and Results

Two procedures were carried out to determine the performance point of the non-linear static analyses, one suggested by the American regulation ATC40 and the other suggested by Eurocode 8, method N2.

A non-linear static analysis was made by applying an incremental load to the structure and recording the displacement suffered at a point on the structure. This point was designated the control point.

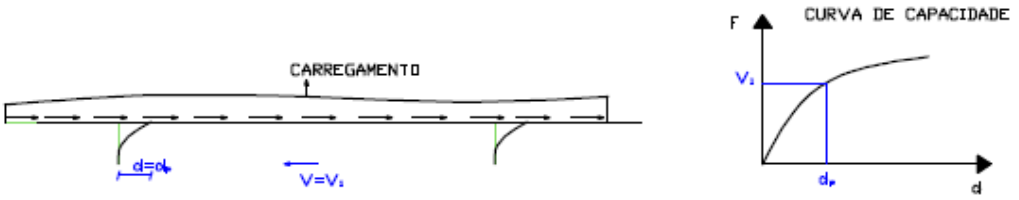

Fig. 9 - Non-linear static analysis representation

The record of the various force–displacement points obtained in the performance of the non-linear static analysis gives the capacity curve. In order to cross-reference this information with the seismic event and determine the performance point, the capacity curve had to be

transformed into its capacity spectrum, i.e. the coordinates of the capacity curve defined in a system of multiple degrees of freedom have to be turned into ADRS coordinates, spectral acceleration–spectral displacement being defined in a system of single degree of freedom, since the response spectra that represent the seismic action are defined for systems with a single degree of freedom.

To determine the performance point of the structure relative to the various seismic events analysed, both procedures used required an iterative process, since the effective damping dissipated by the structure must be equal to the damping introduced into the reduction factor of the response spectra.

It is at this point that the contribution of the viscous dampers on the Padre Cruz viaduct was taken into account. As the constitutive relation of these devices is a relation that depends on velocity and the analysis made was static, in order to calculate the effect of these devices, the first step was to relate the velocity with the displacement. Thus, for a cycle of a vibration period with maximum displacement equal to a possible performance point, the graphic force–displacement could be obtained, which reflects the force that the devices exert for each displacement suffered by the deck.

The constitutive relation of the viscous dampers on the viaduct is of the type

$$F = 4000 \times |v|^{0,1} \times Sinal(v)$$

Starting from the hypothesis that the maximum displacement of the deck for energy purposes is of the perfect harmonic type, the displacement in the piston of the devices is yielded by the next expression:

$d(t) = Asen(pt)$ and knowing that $v(t) = \frac{d(d(t))}{dt} = pAcos(pt)$

Where *A* is the maximum displacement of an ideal cycle and *p* is the value of the first-mode vibration frequency in a longitudinal direction.

Thus, a velocity is associated with each displacement, and knowing the velocity the corresponding force is calculated and the force–displacement relation referring to the set of viscous dampers is built up.

To calculate the effective damping of the structure and viscous damper system, all that remains is to add up the relation obtained earlier and the possible hysteresis loops relating to the deformation of the structure. These loops are idealised on the basis of the capacity curve obtained from the non-linear static analyses. See figure 10.

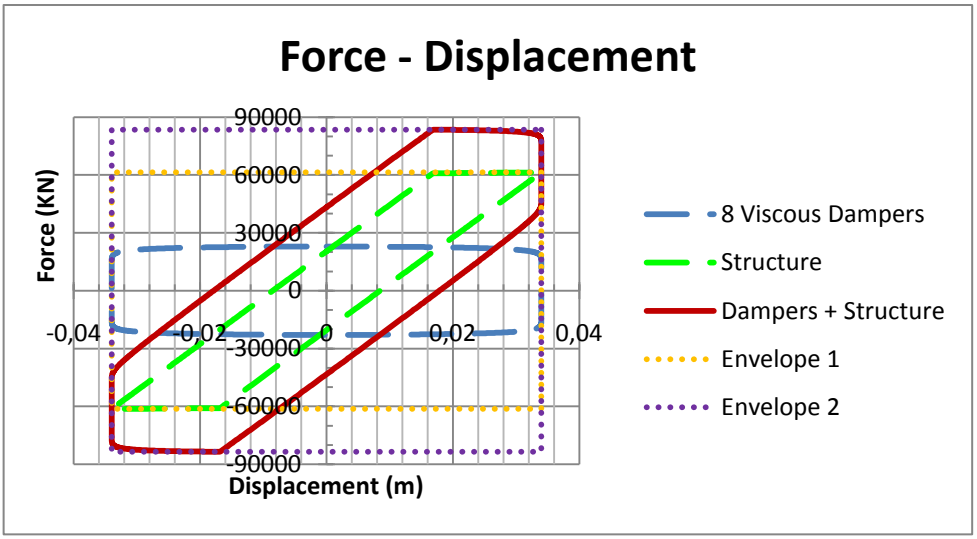

Fig. 10 - Hysteresis loops

The effective damping is given by Chopra's expression with a supplemental viscous damping that depends on the type of material in the structure, +5% for reinforced concrete structures.

$$\zeta_{eff} = \frac{2}{\pi} \times \frac{A_{Dampers\ +Structure}}{A_{Envelope\ \ 2}}$$

Part of the results obtained in this work are represented graphically as follows in figure 11 and 12.

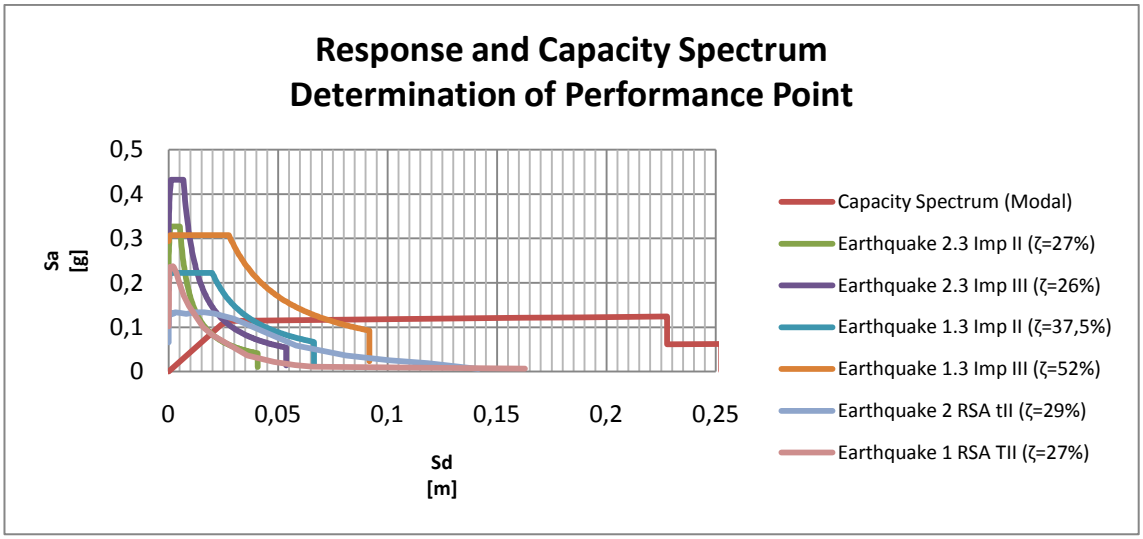

Fig. 11 - Longitudinal results

In the longitudinal direction, the structure shows performance points at the post-yield section but these points are some distance from the point where the first plastic hinge is formed.

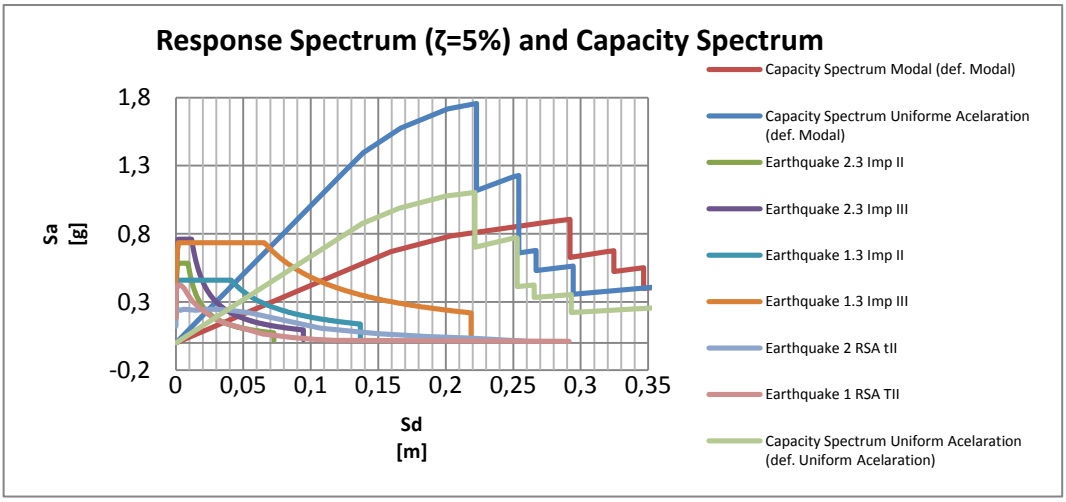

Fig. 12 - Transverse direction results

For the transverse direction, it was observed that for all the seismic events analysed, the structure should respond in a linear way.

7. Fragility Curves

The aim of the final phase of this work was to extrapolate the results obtained from the analyses carried out in order to be able to predict the level of damage the structure might suffer under a given earthquake loading.

For this, the fragility curves were calculated. These curves have a distribution of the log-normal type and reflect the probability of reaching a certain level of damage based on a reference value for seismic activity. For the purpose of this study, this value refers to the spectral acceleration that a seismic event has for the vibration period T=1s and a damping of 5%.

Points on the capacity spectrum were defined that characterise the levels of damage, and the value was determined for spectral acceleration for a period T=1s and 5% damping for the most influential seismic activity, which has as a performance point a given level of damage, this value corresponding to the median fragility curve that defines the level of damage obtained as performance point. Thus, all the fragility curves were built up.

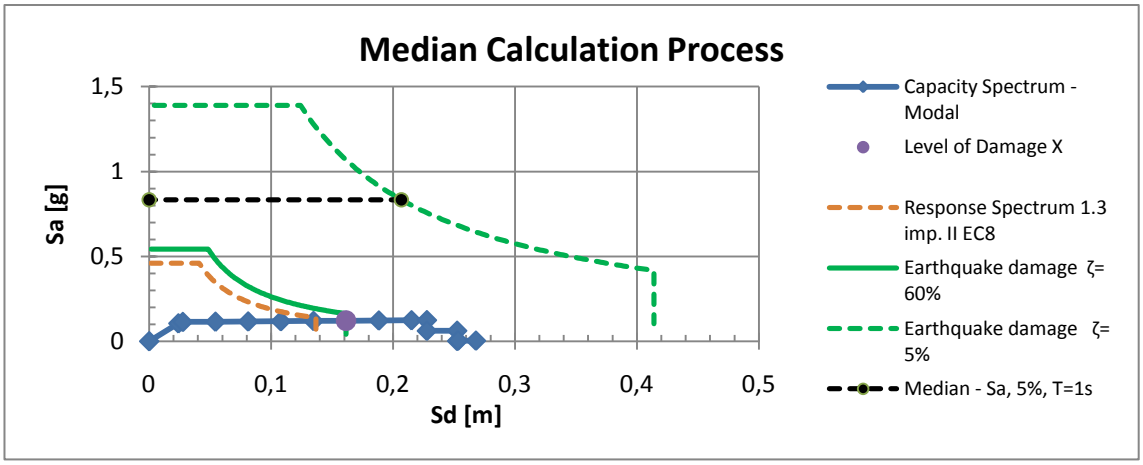

Fig. 13 - Representation of the median calculation process

8. Conclusions

The Padre Cruz viaduct was dimensioned for the seismic actions defined in the RSA. As would be expected, the structure should not reach collapse under this regulation. However, since the regulations in force in 2010 will be those defined by Eurocodes, the response of the viaduct was checked when subjected to seismic events regulated under EC8, which are more stringent than those in the RSA, and it was observed that for any horizontal direction the structure is safe and should not collapse.

In the more rigid, transverse direction, the structure should respond under a linear regime to any earthquake loading considered. As for the longitudinal direction, the structure could enter into a non-linear regime but the performance points for all events are quite distant from the point where the structure forms the first plastic hinge. This great distance is achieved by using 8 viscous dampers.

It is important to point out that analyses on the viaduct were also carried out ignoring the presence of the viscous dampers, and it was concluded that the structure should not collapse either; however, performance points are more closer to the point where the first plastic hinge is formed, so it could be concluded that in this case the structure will show much greater plastic deformations, significantly increasing the damage.

The results of the N2 and ATC40 methods are similar.

We conclude that the methodology proposed in this study is simple and practical when what is required is to quantify the presence of viscous dampers in non-linear static analyses, thus avoiding the need to carry out non-linear dynamic analyses since these present a high degree of complexity.